

AIAA 81-0223R

Flight Instabilities of Spinning Projectiles Having Nonrigid Payloads

Miles C. Miller*

Chemical Systems Laboratory—ARRADCOM, Aberdeen Proving Ground, Md.

Severe flight instabilities were experienced by an Army spin-stabilized projectile which had a partial-solid/partial-liquid payload. Characteristic of this flight instability was a sharp increase in projectile yaw angle accompanied by an abrupt loss in projectile spin rate. It was known that this instability was due to movement of the nonrigid payload, but the exact mechanism causing the effect was not understood. A special laboratory test fixture was used to force a full-scale projectile payload to simulate the combined spin and simple coning motion of the projectile in flight. The fixture was used to determine critical factors influencing the payload-induced despin moment, and from this the associated flight stability was inferred. Candidate payload configurations intended to eliminate the instability were evaluated on the fixture, culminating in a payload design which provided the desired functional and flight performance. Subsequent fixture tests with homogeneous, viscous liquid fills produced similar despin characteristics to those obtained with the partial-solid/partial-liquid payloads. The despin data indicated increasing instability with increasing liquid viscosity with a maximum effect at a kinematic viscosity of about 10^5 CS whereupon the instability decreases with increasing viscosity. Instrumented flight tests showed good correlation with fixture results. The similar instability characteristics of the homogeneous, viscous liquids and the partial-liquid/partial-solid payloads could aid in developing a general theory describing this instability.

Nomenclature

I_C	= canister and payload axial moment of inertia
I_P	= projectile total axial moment of inertia
M	= despin moment due to nonrigid payload
M_{AERO}	= despin moment due to aerodynamic effects
M_F	= despin moment due to canister bearing friction
M_A	= despin moment due to air turbine
p	= spin rate of projectile
$SIGMA N$	= angle of projectile centerline relative to sun direction
t	= time
WP	= white phosphorus
α	= nutation yaw angle
γ	= specific mass density
θ	= test fixture canister coning angle
μ	= kinematic viscosity
Ω	= test fixture canister coning rate
ω	= test fixture canister spin rate
ω_N	= nutation frequency
($\dot{}$)	= denotes time derivative

Introduction

THE use of an artillery delivered smoke screen has received new impetus as a means of reducing the vulnerability of friendly forces to enemy weapons, particularly guided missiles. The XM761, 155-mm artillery projectile was intended to provide an improved smoke screening capability. The round consisted of an M483A1-type projectile body containing a preloaded payload canister assembly illustrated in Fig. 1.

The thin-walled, aluminum payload canister shown in Fig. 2 had an inside length of 51.76 cm and an inside diameter of 12.06 cm. An aluminum cruciform baffle ran the length of the cylinder, effectively dividing the interior into four quadrants. A total of 48 cotton patio torch wicks was placed in the canister in three tiers with 16 wicks per tier. A single wick

(also shown in Fig. 2) measured about 16.5 cm in length and weighed about 17 g. The canister was then filled with liquid WP, resulting in the wicks being saturated with WP. The fully loaded canister had a mass of 12.25 kg including 5.8 kg of WP, giving a total projectile weight of about 46.27 kg.

The wicks retained the WP, whether in a liquid (hot) or solid (cold) state. Upon expulsion from the projectile over the target, the WP-saturated wicks would be dispersed onto a relatively large area of the ground. Each wick would spontaneously ignite, providing a series of point sources of smoke resulting in a rapidly formed, dense smoke screen of relatively long duration.

The XM761 projectile produced the desired smoke screening performance. However, during the subsequent development program, flight tests revealed a serious flight stability problem.¹⁻³

When fired at a low temperature with the WP in a solid state, the projectiles had stable flights under all launch conditions. Figure 3 contains yawsonde data for a typical stable flight. The peak-to-peak amplitude of the SIGMA N trace denotes the total angle of yaw possessed by the projectile. A reduction of yaw with time represents a stable projectile flight, whereas an increasing yaw with time would indicate an unstable condition.

At elevated temperatures where the WP was in a liquid state, the projectile experienced a severe flight instability. The unique feature of this instability was that both a large increase in yaw angle and severe loss in spin rate were suffered by the projectile, causing the round to fall short of its intended range. This problem was particularly critical at the Zone 4 (transonic muzzle velocity) firing condition where the projectile possesses minimum aeroballistic stability and experiences relatively large initial yaw angles. Figure 4 presents yawsonde data from a typical unstable flight and clearly depicts the increase in yaw angle and simultaneous loss in spin rate. The test data indicated that the nutation rate and angle are the critical motions with regard to this unstable behavior.

A similar type of flight instability which produces coupling between yaw and spin had been recently identified and documented. Aeroballistic analysis of that problem indicated that rotational motion of the projectile in flight caused rigid components internal to the projectile to assume specific

Presented as Paper 81-0223 at the AIAA 19th Aerospace Sciences Meeting, St. Louis, Mo., Jan. 12-15, 1981; submitted March 2, 1981; revision received July 23, 1981. This paper is declared a work of the U.S. Government and therefore is in the public domain.

*Chief, Aerodynamics Research and Concepts Assistance Section, Physics Branch, Research Division. Member AIAA.

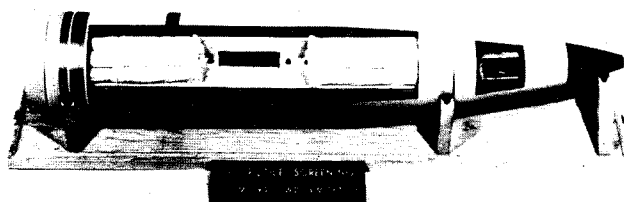


Fig. 1 XM761 projectile and payload arrangement.

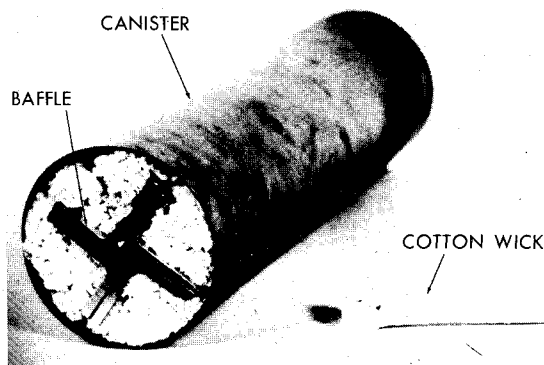


Fig. 2 XM761 payload canister and wick.

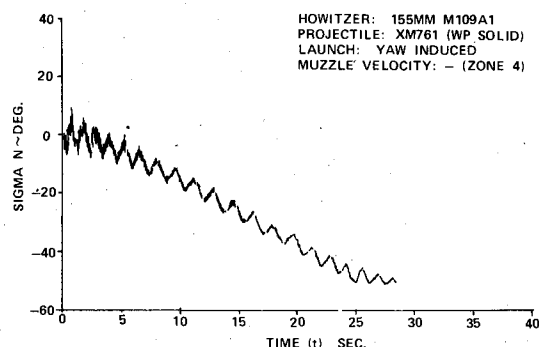
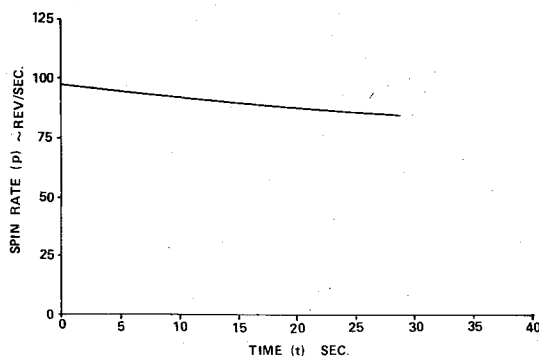


Fig. 3 Yawsonde data for XM761 stable flight (WP solid).

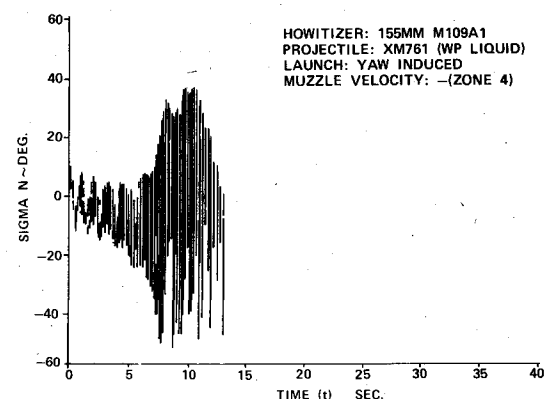
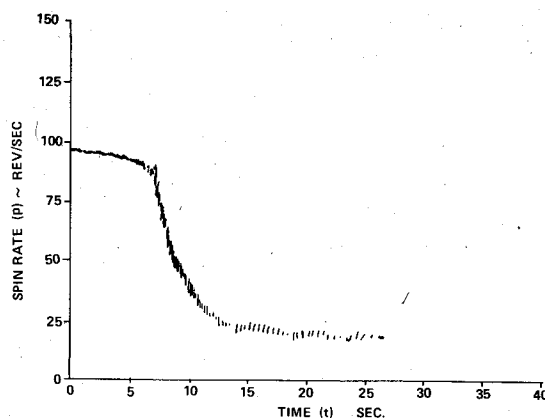


Fig. 4 Yawsonde data for XM761 unstable flight (WP liquid).

Accordingly, a special ground test fixture was built which caused an actual, full-scale projectile payload assembly to undergo the basic spin and nutation motion of the projectile in flight.⁵ The internal payload motion could then be reproduced, the resulting despin moment measured, and the data used to evaluate the potential flight stability of the projectile carrying the payload configuration tested.

This paper describes the use of this laboratory test fixture to determine the critical performance characteristics of the despin resulting from the relative motion of the XM761-type nonrigid payload; the subsequent use of the fixture to evolve a stable WP smoke round payload configuration; and the results of studies with simple homogeneous, viscous liquid fills which demonstrated their similarity of the more complex partial-solid/partial-liquid nonrigid payloads.

Laboratory Test Fixture Rationale

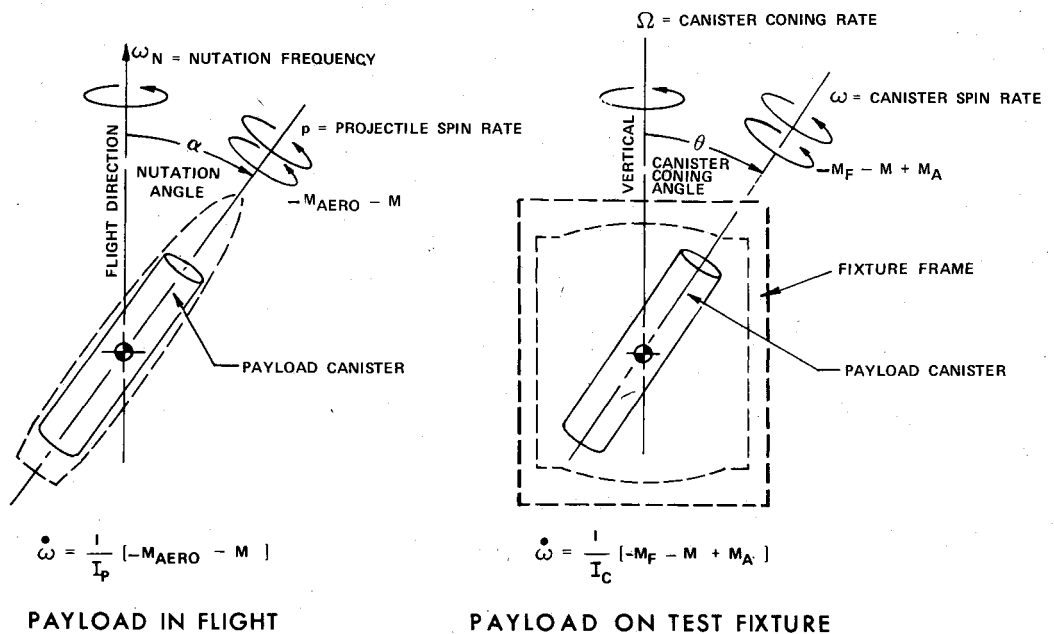
The rationale for the test fixture is based on the assumption that both the yaw moment and spin moment produced by this instability are components of a single payload-induced moment. The spin fixture measures only the despin component of the total destabilizing moment induced by the nonrigid payload. Assessment of the destabilizing potential of a particular payload is based on the premise that a payload-induced destabilizing yawing moment is present that is proportional to the magnitude of the payload-induced despin moment measured on the test fixture.

A better understanding of this situation can be gained by comparison with other types of flight instabilities. In the case of a Magnus instability which is due to an external aerodynamic effect, the resulting instability moment acts about an axis which is perpendicular to the spin (longitudinal) axis of the projectile. Thus only the yaw of the projectile is affected. A Stewartson-type⁶ instability is caused by an internal pressure wave effect in a pure liquid payload. However,

motions relative to the projectile body, producing an inertial moment which affected the flight stability of the projectile. Murphy⁴ subsequently produced a detailed theory describing the specific cause of this inertial effect, which was based on rigid, well-defined components located within the projectile.

The flight instabilities of the XM761 projectile appeared to be similar, but were more severe. However, because of the nonrigid composition of the payload components of the XM761 projectile (i.e., partial solid/partial liquid), no theory existed for this particular situation.

Fig. 5 Test fixture rationale.



the resulting instability moment axis is also perpendicular to the projectile spin axis and only affects the projectile yawing motion. The moment produced by an inertial instability due to an internal moving part acts about an axis which is not perpendicular to the projectile longitudinal axis. Thus the component of this moment perpendicular to the longitudinal axis affects the yaw of the projectile, while the component parallel to the longitudinal axis acts to despin the projectile. Because of the similarities in the unstable projectile motion of the XM761 and that produced by an inertial instability, it was assumed that the single moment effect was a common factor in both types of instabilities even though the exact mechanism producing the moment might not be the same.

Figure 5 compares the motion and moments acting on the projectile in flight with those experienced by the payload canister in the laboratory test fixture. As shown in Fig. 5a, the projectile has a spin rate about its longitudinal axis and is assumed to be undergoing simple coning motion with a nutation frequency and at a nutation angle. The rotational motion assumed by a spinning projectile in flight includes both precessional (slow frequency) and nutational (fast frequency) epicyclic motion. However, it had been determined from flight test data that the nutational motion appeared to be the major factor in the instability. Thus, simple nutational coning motion was regarded as a valid and sufficient representation of the projectile flight motion with regard to its influence on the payload motion and its resulting despin moment. In flight, the spin rate of the projectile and the enclosed payload canister is a function of two moments: the external aerodynamic spin damping moment and the payload-induced despin moment, as shown.

The laboratory test fixture arrangement is shown in Fig. 5b. Since the instability being studied is due solely to an internal payload effect, the external projectile shaping is not required. It is only necessary to match the payload elements and their internal constraints. These characteristics are present because an actual canister and payload assembly are used. The canister is attached to the fixture frame by bearings, allowing it to spin freely about its longitudinal axis, while the fixture frame is forced to spin about a vertical axis. This results in the canister assuming the desired simultaneous spinning and coning motion similar to that of the projectile in flight. In the case of the test fixture, the spin rate of the canister is the net result of three moments: an air turbine moment which causes the canister to attain its spin, a friction moment due to the canister bearings, and the payload-induced despin moment.

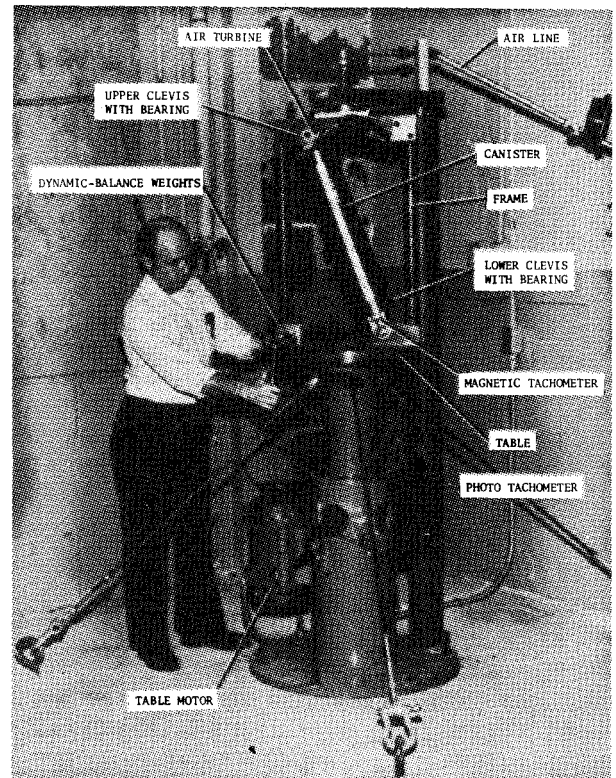


Fig. 6 Laboratory test fixture.

The friction moment and turbine moment are effects which are only present in the test fixture, and their values are determined by calibration. Therefore the spin deceleration of the coning canister can be used to determine the payload-induced despin moment.

Description and Operation of the Laboratory Test Fixture

Figure 6 contains a photograph of the laboratory test fixture showing the system details. An actual, full-scale canister and enclosed payload assembly from a 155-mm projectile is mounted between two clevis assemblies, each

containing a bearing. These clevises are mounted to the test fixture frame so that the canister longitudinal axis can be oriented at a predetermined angle to the vertical. This angle represents the nutational coning angle. The canister can be set at angles from 0 to 20 deg in 5-deg increments. The upper clevis contains a nozzle/air turbine arrangement providing spin torque to the canister. The table, frame, and attached canister are rotated about a vertical axis by means of an electric motor located on the lower section of the test fixture. The canister spin rate is measured by means of a magnetic tachometer located on the lower clevis, whereas the table spin (coning) rate is indicated by a phototachometer located beneath the table. Weights located on opposite corners of the frame eliminate dynamic imbalance effects due to the canister angle.

A typical test run sequence is as follows: with the canister mounted at a particular angle, the air turbine spins the canister up to the spin rate of the projectile for the specific conditions being tested; approximately 60 s being required to achieve 6000 rpm. When the desired canister spin rate has been achieved, the electric motor spins the table with the attached frame and spinning canister up to the desired nutational coning frequency. When the canister has reached a constant coning rate, the air turbine is cut off, allowing the canister to spin down due to the combined effects of bearing friction and the payload-induced despin moment. The canister spin rate is recorded as a function of time. The total canister despin moment at a particular canister spin rate and coning rate can be determined by multiplying the spin deceleration measured at that condition by the total canister axial moment of inertia. The despin moment due to friction is known from previous calibration as a function of the canister spin rate, coning rate, and coning angle. Therefore any additional despin moment is due to a payload-induced effect. Similarly, tests could be conducted over a range of constant coning rates at each fixed coning angle, thus encompassing nutation rates corresponding to various firing zones and initial yaw angles.

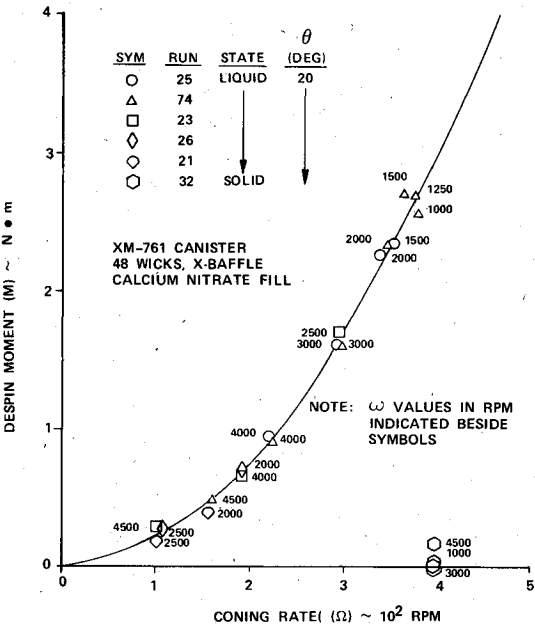
Evaluation of the XM761 Payload

A series of tests were conducted on the test fixture using an actual XM761 canister assembly containing 48 patio torch wicks, the cruciform-longitudinal baffle, and calcium nitrate as a simulant for WP. Calcium nitrate is the commonly used simulant for WP because it has the same mass density and melting temperature. The canister was evaluated with the WP simulant in both a solid (cool) and a liquid (hot) state.

For a given canister angle, the despin moment was plotted as a function of the coning rate, as shown in Fig. 7. Data from several runs for the same canister configuration are shown. The numbers beside each symbol indicate the spin rate of the canister for the particular data point. The despin moment was not a function of canister spin rate, provided a sufficient canister spin rate is present ($\omega > 1000$ rpm) and can be represented by a single curve as shown. The data indicate that the despin moment is a nonlinear function of the coning rate. It should also be noted that tests with a solid payload produced no payload-induced despin moment. This testing procedure was repeated at canister angles of 15, 10, and 5 deg, resulting in the data shown in Fig. 8. These data are presented in a different form in Fig. 9, which contains the despin moment as a function of canister coning angle for various

coning rates and indicates that the despin moment is a nonlinear function of the coning angle.

The test fixture results revealed that the payload-induced despin moment is not dependent on set-back (longitudinal acceleration) at launch. This latter fact was important in that payload asymmetries created by the projectile yaw ac-



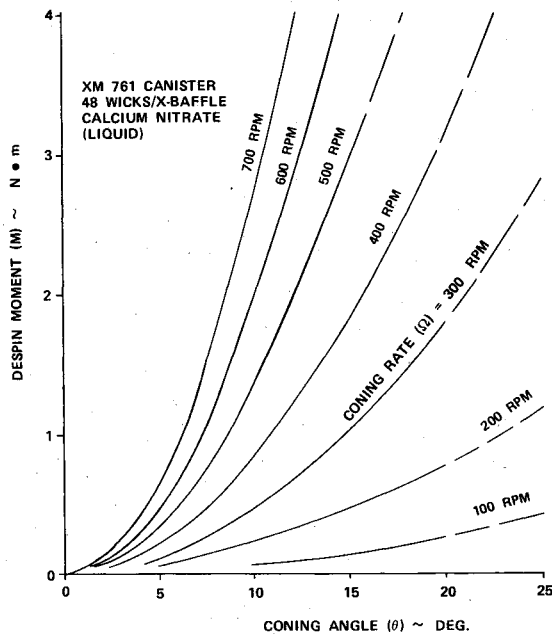


Fig. 9 Despin moment for the XM761 payload as a function of coning angle and coning rate.

celeration at launch had initially been considered to be a possible cause of the instability. Also, the payload-induced despin could be reproduced even after a liquid/solid/liquid cycle and thus is not a one-time, irreversible effect.

The despin data obtained from the fixture showed good correlation with projectile spin loss measured during flight tests, providing confidence that the fixture could be used to access the potential flight performance of candidate payload configurations.

Evolution of XM825 Configuration

With the basic capabilities demonstrated, the test fixture was used to evaluate several candidate payload canister configurations in support of the ARRADCOM, Chemical Systems Laboratory (CSL) efforts to evolve an improved 155-mm WP smoke round.

An initial investigation was performed to evolve a simulant for WP that would be liquid at room temperature. The result was a blend of two inert and nontoxic E-series Freons providing a close match of the basic physical properties of liquid WP, including the specific density and specific viscosity (Table 1), and did not require the elevated temperatures for liquid-state tests as does the calcium nitrate.

Fixture tests conducted with the nominal XM761 payload configuration, but using the blended Freon simulant, produced identical despin moments to those obtained with the same payload configuration using calcium nitrate as the simulant, thereby validating the blended Freon as a simulant for liquid WP. The use of the blended Freon and a reusable canister greatly simplified the testing procedure and reduced the time involved in the subsequent test program.

Various payload configurations were evaluated on the fixture. Despin moments due to the nonrigid payloads were measured on the fixture even with payload configurations which had demonstrated stable flight characteristics. It would appear that the projectile possesses sufficient inherent aeroballistic stability to overcome a certain degree of this payload-induced stability. However, if the payload-induced effect is large enough, it will dominate and cause the projectile to become unstable.

A configuration was evolved by the ARRADCOM, CSL composed of ninety-two 1-in.-thick F7-type felt wedges which were stacked between the cruciform-longitudinal baffle as illustrated in Fig. 10. The felt wedges served the same function

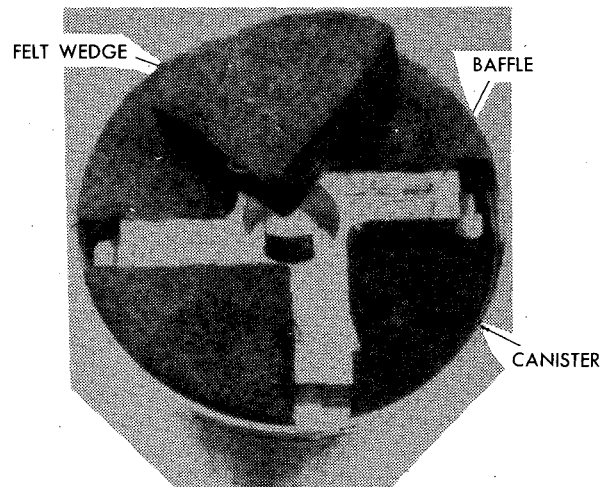


Fig. 10 XM825 felt wedge payload configuration.

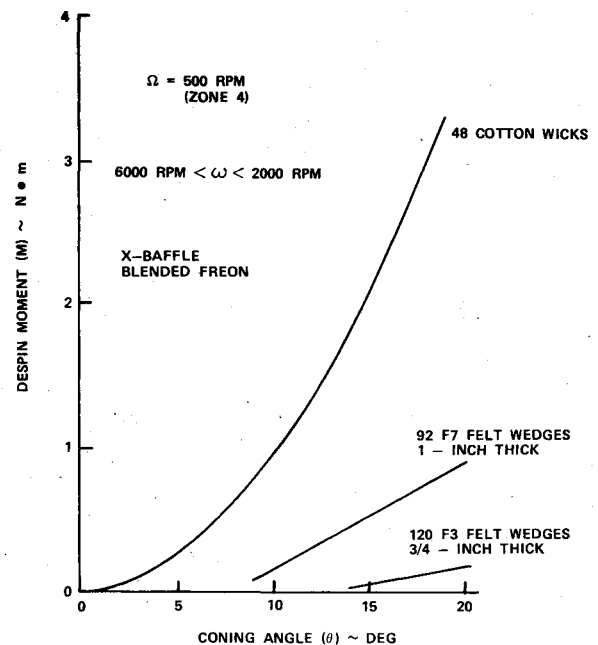


Fig. 11 Comparison of despin moment for cotton wick (XM761) and felt wedge (XM825) payloads.

as the cotton wicks, but the denser material and tighter packing of the felt wedges restricted their movement inside the canister. Test fixture results for this payload configuration are shown in Fig. 11 and indicate a despin moment considerably lower than that measured for the nominal XM761. Data are shown for a coning rate of 500 rpm which is the projectile nutational frequency for the critical Zone 4 (transonic launch) condition. Subsequent flight tests of the felt wedge configuration using actual liquid WP resulted in stable flights under firing conditions which cause the nominal XM761 WP/wick configuration to be unstable.⁷

The test fixture was then used to evaluate alternate felt wedge sizes, materials, and packing densities. A payload configuration composed of 120 3/4-in.-thick, higher density F3-type felt wedges resulted in a significantly lower despin moment (Fig. 11), indicating improved stability characteristics. This latter performance was also subsequently demonstrated in instrumented flight tests.⁸ Based on the improved flight stability, this latter configuration was entered into development as the XM825 projectile.

Evaluation of Homogeneous Viscous Liquid Fills

Although the original goal of the laboratory spin fixture was achieved in the evolution of the improved smoke screening projectile, the exact source of the instability associated with this partial-solid/partial-liquid type of nonrigid payload was still not understood. The fixture was next used to generate a data base to provide further insight into the physical phenomena responsible for the instability.

Vaughn⁹ proposed a hypothesis that the combined solid/liquid XM761 payload acts as a homogeneous, highly viscous liquid. An extensive series of controlled experiments was conducted with the laboratory test fixture using liquid fills of various viscosities and densities both with and without the baffle.¹⁰ The liquids were selected to represent various viscosity ranges. Different viscosity values for a given liquid were achieved by preconditioning the liquid to a specific temperature. These tests indicate that a cylindrical canister, completely filled (i.e., no void) with a homogeneous viscous liquid produces a measurable payload induced despin moment under the combined spinning and coning motion of the test

fixture. Figure 12 contains representative data for the canister (without baffle) filled with corn syrup having a specific mass density of 1.4 and a kinematic viscosity of 200,000 CS. The despin moment was found to be independent of canister spin rate for the range of spin rate values considered. Also, the payload-induced moment is a nonlinear function of both the coning rate and coning angle. The similarities of these results with the data for the XM761 payload are apparent.

Figure 13 shows the despin moment as a function of the liquid fill kinematic viscosity for a 20-deg canister coning angle. It had been determined from these tests that the despin moment is directly proportional to the liquid density. Accordingly, the despin moment has been normalized to the mass density of water. These data show that for the 100%-filled cylindrical canister (without baffle) the design increases

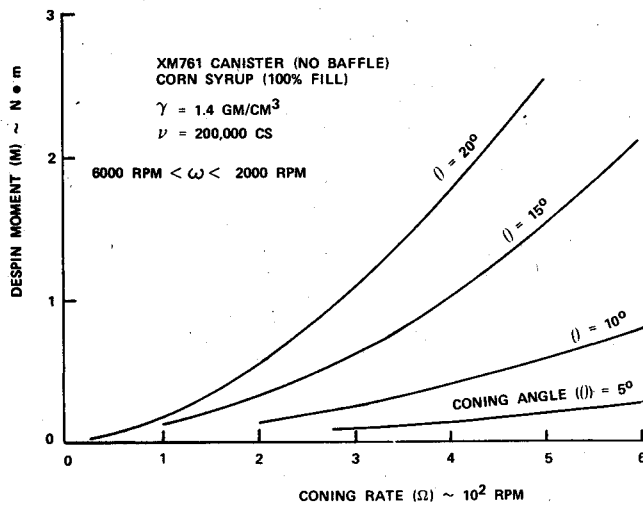


Fig. 12 Despin moment for a homogeneous high-viscosity liquid as a function of coning rate and coning angle.

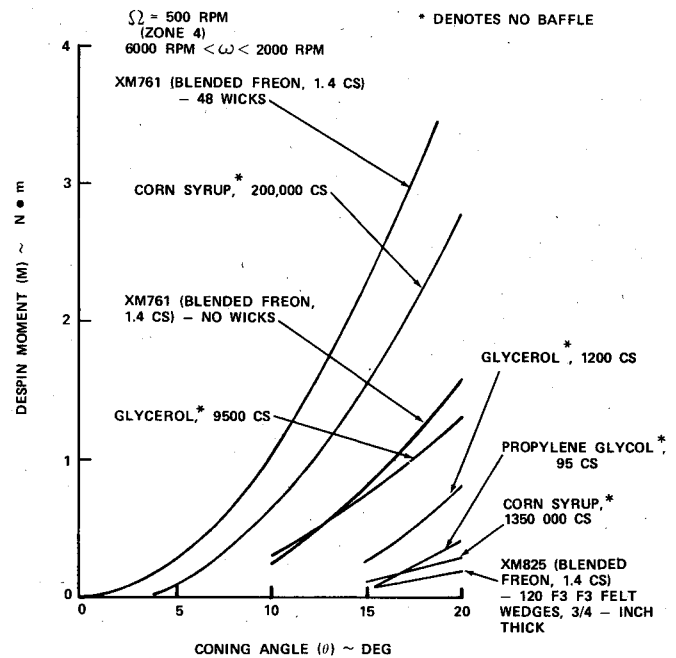


Fig. 14 Despin moment as a function of coning angle for selected nonrigid payload configurations.

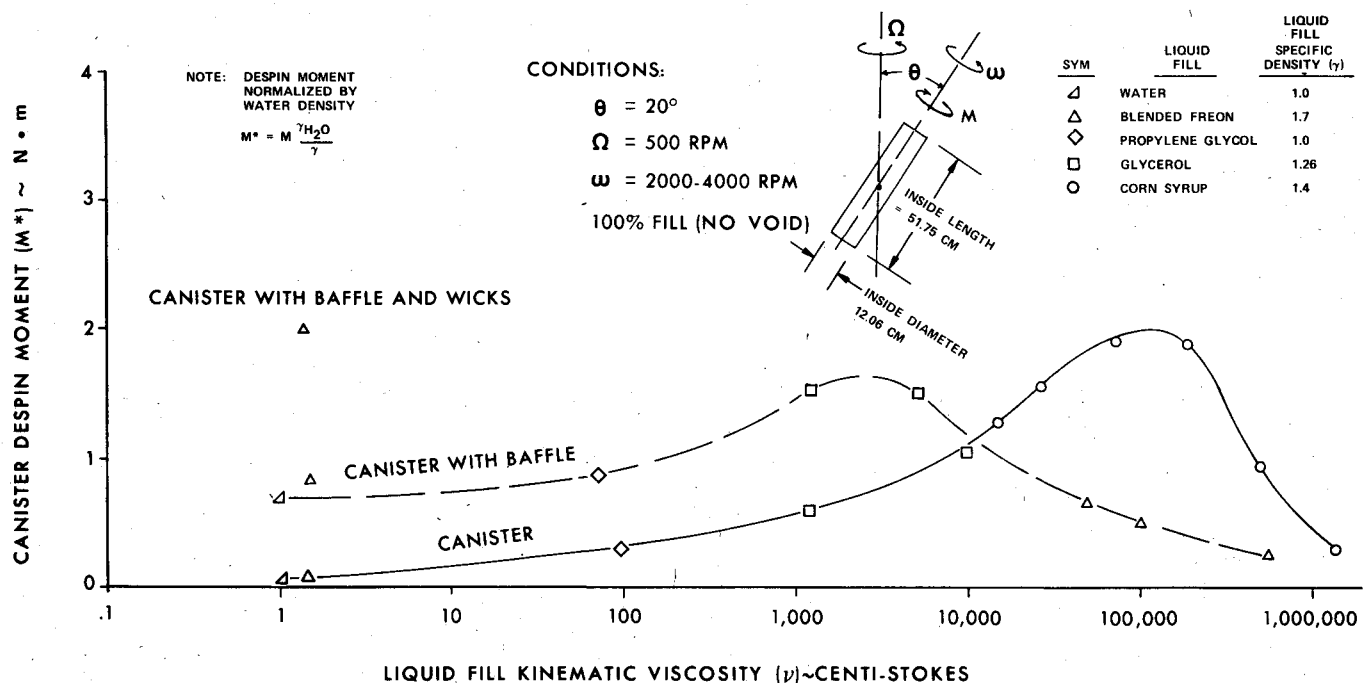


Fig. 13 Despin moment as a function of liquid fill kinematic viscosity for a 20-deg coning angle.

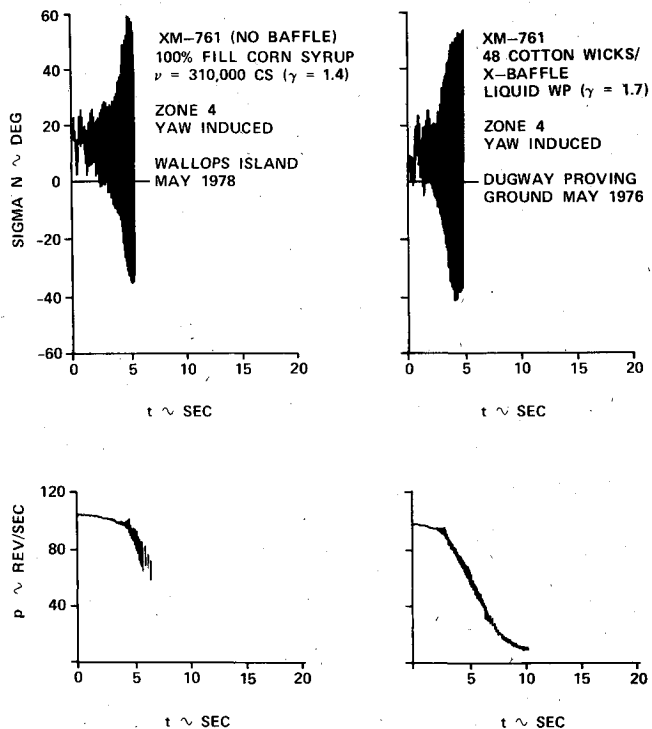


Fig. 15 Comparison of the unstable flight motion of a 155-mm projectile having a homogeneous viscous liquid fill and a partial-liquid/partial-solid payload (XM761).

with the liquid fill viscosity, achieving a maximum value in the 10^5 CS range, thereupon diminishing to zero at very large values of viscosity. The presence of the cruciform-longitudinal baffle with a given liquid results in a despin moment equivalent to that of a pure liquid of higher viscosity and remains at a constant level at the lower viscosity range.

Figure 14 presents selected test fixture data for several homogeneous, viscous liquids as well as for the partial-liquid/partial-solid payloads of the XM761 and XM825. These data illustrate additional characteristics which are not apparent in the generalized, single coning angle data of Fig. 13. Note that for the homogeneous liquids having viscosities less than or greater than the 10^5 CS range of the peak design value, the payload-induced despin moment is only present at the larger coning angles.

The magnitude of the despin moment measured for the canister filled with corn syrup ($\nu=200,000$ CS) is nearly identical to that of the XM761 payload configuration. Thus, based on these results, a projectile filled with corn syrup should experience a similar flight instability. Subsequent instrumented flight tests of full-scale 155-mm projectiles having identical viscous liquid payloads to those evaluated on the test fixture were conducted by the Ballistic Research Laboratory.^{11,12} These tests showed good qualitative correlation to the fixture results. The similarity between the unstable flight motion of a corn-syrup-filled projectile and that of the XM761 is apparent from Fig. 15.

This similarity could mean that the instabilities are due to a common source. If true, a theoretical analysis based on a well-defined homogeneous viscous liquid fill might be more tractable than for the more difficult to quantify partial-liquid/partial-solid-type nonrigid payloads.

Conclusions

1) A laboratory test fixture forces full-scale 155-mm nonrigid payload assemblies to undergo the combined spinning and simple coning motion of the projectile in flight. The despin moment produced by the nonrigid payload under these motion conditions is measured and used to evaluate the potential flight stability of a projectile carrying the nonrigid payload.

2) Test fixture evaluation of the partial-solid/partial-liquid payload indicates that the payload-induced despin moment increases nonlinearly with both coning frequency and coning angle. The despin moment is independent of canister spin rate providing a minimum spin rate of about 1000 rpm is present. Below this spin rate, the despin moment is markedly decreased. Modifying the shaping and composition of the solid elements of the payload to restrict their movement reduced the despin moment and the associated flight instability potential.

3) Fixture tests with homogeneous, viscous liquid fills produced similar despin characteristics to those obtained with the partial-solid/partial-liquid payloads. These data indicate increasing instability with increasing liquid viscosity with a maximum effect at a kinematic viscosity of about 10^5 CS, whereupon the instability decreases with increasing viscosity. The despin moment was found to be directly proportional to the liquid mass density.

4) The similarity in the instability characteristics due to both the simple homogeneous, viscous liquids and the more complex partial-solid/partial-liquid nonrigid payloads could aid in the development of a general theory describing the source of the instability and establishing design criteria for future projectile applications.

References

- 1 D'Amico, W.P., "Early Flight Experiments With the XM761," Ballistic Research Laboratory Memo. Rept. 2791, Sept. 1977.
- 2 D'Amico, W.P., "Field Tests of the XM761: First Diagnostic Test," Ballistic Research Laboratory Memo. Rept. 2792, Sept. 1977.
- 3 D'Amico, W.P., "Field Tests of XM761: Second Diagnostic Test," Ballistic Research Laboratory Memo. Rept. ARBRL-MR-02806, Jan. 1978.
- 4 Murphy, C.H., "Influence of Moving Internal Parts on Angular Motion of Spinning Projectiles," *Journal of Spacecraft and Rockets*, Vol. 1, March-April 1978, pp. 117-122.
- 5 Miller, M.C., "Flight Instability Test Fixture for Non Rigid Payloads," U.S. Army Research and Development Command Report, ARRADCOM Special Publication ARCSL-SP-79005, Jan. 1979.
- 6 Stewartson, K., "On the Stability of a Spinning Top Containing Liquid," *Journal of Fluid Mechanics*, Vol. 5, Part 4, June 1959, pp. 577-592.
- 7 D'Amico, W.P., "Aeroballistic Testing of the XM825 Projectile: Phase I," Ballistic Research Laboratory Memo. Rept. ARBRL-MR-02911, March 1979.
- 8 D'Amico, W.P. and Oskay, V., "Aeroballistic Testing of the XM825 Projectile: Phase II," Ballistic Research Laboratory Interim Memo. Rept. ARBRL-IMR-679, March 1980.
- 9 Vaughn, H.R., "Flight Dynamic Instabilities of Fluid Filled Projectiles," Sandia Laboratories, Albuquerque, N.Mex., SAND 78-0999, June 1978.
- 10 "In-House Laboratory Independent Research Program (ILIR)-Annual Review FY78," U.S. Army Chemical Systems Laboratory Special Rept. ARCSL-SR-79003, Oct. 1978, pp. 3, 1-9.
- 11 D'Amico, W.P. and Miller, M.C., "Flight Instability Produced by a Rapidly Spinning, Highly Viscous Liquid," *Journal of Spacecraft and Rockets*, Vol. 16, Jan.-Feb. 1979, pp. 62-64.
- 12 D'Amico, W.P. and Clay, W.H., "High Viscosity Liquid Payload Yawsonde Data for Small Launch Yaws," Ballistic Research Laboratory Memo. Rept. ARBRL-MR-03029, June 1980.